

## Macroscopic Ionic Flow in a Superionic Conductor $\text{Na}^+$ $\beta$ -Alumina Driven by Single-Cycle Terahertz Pulses

Yasuo Minami<sup>1,2,\*</sup>, Benjamin Ofori-Okai<sup>3</sup>, Prasahnt Sivarajah,<sup>3</sup> Ikufumi Katayama<sup>2</sup>, Jun Takeda<sup>2</sup>,  
Keith A. Nelson,<sup>3</sup> and Tohru Suemoto<sup>4</sup>

<sup>1</sup>*Department of Industrial and Social Sciences, Tokushima University, Tokushima 770-8506, Japan*

<sup>2</sup>*Department of Physics, Faculty of Engineering Science, Yokohama National University, Yokohama 240-8501, Japan*

<sup>3</sup>*Department of Chemistry, Massachusetts Institute of Technology, Massachusetts 02139, USA*

<sup>4</sup>*Toyota Physical and Chemical Research Institute, Nagakute, Aichi 480-1192, Japan*



(Received 31 January 2020; accepted 28 February 2020; published 9 April 2020)

Ionic motion significantly contributes to conductivity in devices such as memory, switches, and rechargeable batteries. In our work, we experimentally demonstrate that intense terahertz electric-field transients can be used to manipulate ions in a superionic conductor, namely  $\text{Na}^+$   $\beta$ -alumina. The cations trapped in the local potential minima are accelerated using single-cycle terahertz pulses, thereby inducing a macroscopic current flow on a subpicosecond timescale. Our results clearly show that single-cycle terahertz pulses can be used to significantly modulate the nature of superionic conductors and could possibly serve as a basic tool for application in future electronic devices.

DOI: [10.1103/PhysRevLett.124.147401](https://doi.org/10.1103/PhysRevLett.124.147401)

Recent advances in ultrashort laser technology have enabled the control of carrier-envelope phases of few-cycle pulses, which play critical roles in nonperturbative, nonlinear phenomena [1–8]. Such studies provide possibilities for petahertz science with attosecond light fields, generation of high harmonics, and field-induced tunneling. However, most of these phenomena are dominated by the ultrafast electron dynamics of materials, and the nonperturbative responses of ions have rarely been investigated. This is because the greater the mass of ions compared to that of electrons, the more difficult it becomes to manipulate these ions over a substantial distance from their equilibrium position. In addition to electron motion, ionic motion is a key factor affecting the atomic arrangements in solids [9]. Thus, it is important to investigate the possibility of controlling the ionic motion in nonperturbative regimes using external light fields.

An intuitive consideration of ionic motion based on the electron–proton mass ratio ( $m_p/m_e \approx 1840$ ) and electron–electron scattering time in femtoseconds (fs) suggests that the dynamics of ions should evolve on picosecond (ps) timescales corresponding to the terahertz frequency range. Therefore, intense phase-locked terahertz waves at sufficiently high field strengths could possibly be used to generate a nonperturbative ionic response, which may be useful for controlling material properties in future electro-ionic devices [10]. To demonstrate the field control of ionic motion, this Letter focuses on a superionic conductor in which the current is normally carried by cations in the periodic potential minima in the lattice. We show that a field-driven ionic motion is induced by applying an intense

terahertz field, generating a macroscopic current that depends on the polarity of the applied terahertz field.

As  $\text{Na}^+$  ion control is one of the key technologies for next-generation power sources, such as rechargeable rare-metal-free batteries [11–13], we investigate stoichiometric crystalline  $\text{Na}^+$   $\beta$ -alumina, which is a superionic conductor wherein  $\text{Na}^+$  ions move in the two-dimensional space between the spinel layers perpendicular to the  $c$  axis [14]. At room temperature, the shape of the energy potential for  $\text{Na}^+$  ion capture can be simply approximated using a cosine function in the ion propagation direction [14], enabling a simplified and intuitive analysis of the ion dynamics.

Figure 1 shows the schematic of the experimental setup used in this study. We used stoichiometric crystalline  $\text{Na}^+$   $\beta$ -alumina as the sample [14,15]. The dimensions of the sample are  $23 \mu\text{m}$  (thickness,  $c$ -axis direction)  $\times 1 \text{ mm}$  (width)  $\times 2 \text{ mm}$  (electrode spacing). The intense terahertz field was generated using a tilted-pulse-front method via a  $\text{LiNbO}_3$  prism [16,17]. The terahertz field strength was varied using a pair of wire-grid polarizers. The terahertz pulse was incident normal to the sample surface, and the polarization of the field was kept parallel to the direction of electrode spacing and perpendicular to the  $c$  axis. As the radius of the terahertz beam incident on the sample is  $0.5 \text{ mm}$ , nearly 40% of the sample was exposed to intense terahertz radiation. The applied terahertz field stimulated the trapped  $\text{Na}^+$  ions at a laser repetition rate of  $1 \text{ kHz}$ , and the resultant terahertz-field-induced direct electric current was measured using an ammeter. The experiments were carried out under a nitrogen atmosphere at room temperature.

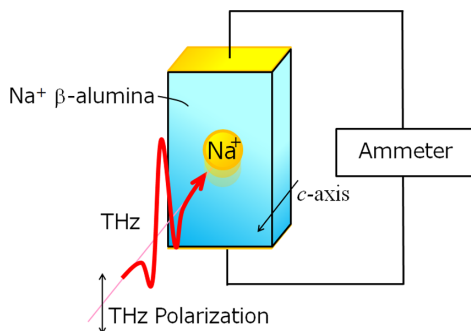


FIG. 1. Setup used for measuring the ionic current induced by the terahertz pulse. The induced macroscopic current is measured using an ammeter. The  $\text{Na}^+$  ions in the sample move in the two-dimensional space between the spinel layers perpendicular to the  $c$  axis.

We applied a terahertz pulse with a peak field strength ranging from 15 to 300 kV/cm. Figure 2(a) shows the dependence of the terahertz-induced direct current on the peak terahertz field strength ( $E$ ) in  $\text{Na}^+$   $\beta$ -alumina. Although the terahertz pulse carries no direct-current components, a terahertz-induced direct current is detected using the ammeter at a high electric field strength. The current is detected only above a threshold field of  $|E| \approx 50$  kV/cm. The maximum current measured is approximately 2 pA, and more importantly, the sign of the current depends on the polarity of the terahertz field. This indicates that the current is neither induced by ionic diffusion nor by electron excitation; in fact, it originates from the direct flow of ions induced by the terahertz electric field. When  $|E| < 50$  kV/cm, the  $\text{Na}^+$  ions vibrate around the local potential minima, as the energy supplied by the terahertz pulse is not high enough to overcome the peak potential barrier [see the left portion of Fig. 2(b)]. Consequently, the  $\text{Na}^+$  ions remain trapped and are immobile, and no current is induced. When  $|E| > 50$  kV/cm, the  $\text{Na}^+$  ions become mobile, as their kinetic energy exceeds the barrier height [see the right portion of Fig. 2(b)]. In this case, the  $\text{Na}^+$  ions move within the sample, inducing a detectable macroscopic current.

To elucidate the change in the ion dynamics observed in the terahertz-induced current measurements, we carried out field-dependent terahertz time-domain spectroscopy measurements. The generated terahertz field is incident on the sample, and the transmitted field is measured using an electro-optic (EO) sampling method [see the left portion of Fig. 3(a)]. Figure 3(b) shows the terahertz field dependence of the energy absorbance. With weak terahertz pulses, the absorption peak is clearly observed on the broad background at  $\sim 1.8$  THz; this peak corresponds to the vibrational mode of the  $\text{Na}^+$  ions oscillating at the bottom of the potential well at room temperature [14]. As the terahertz field strength increases, the peak drastically diminishes before finally vanishing at  $E \approx 300$  kV/cm. To better understand this result, we plot the field dependences of the normalized

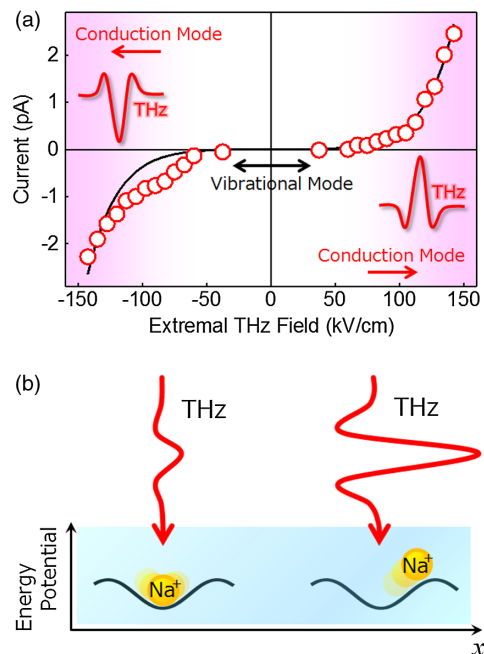
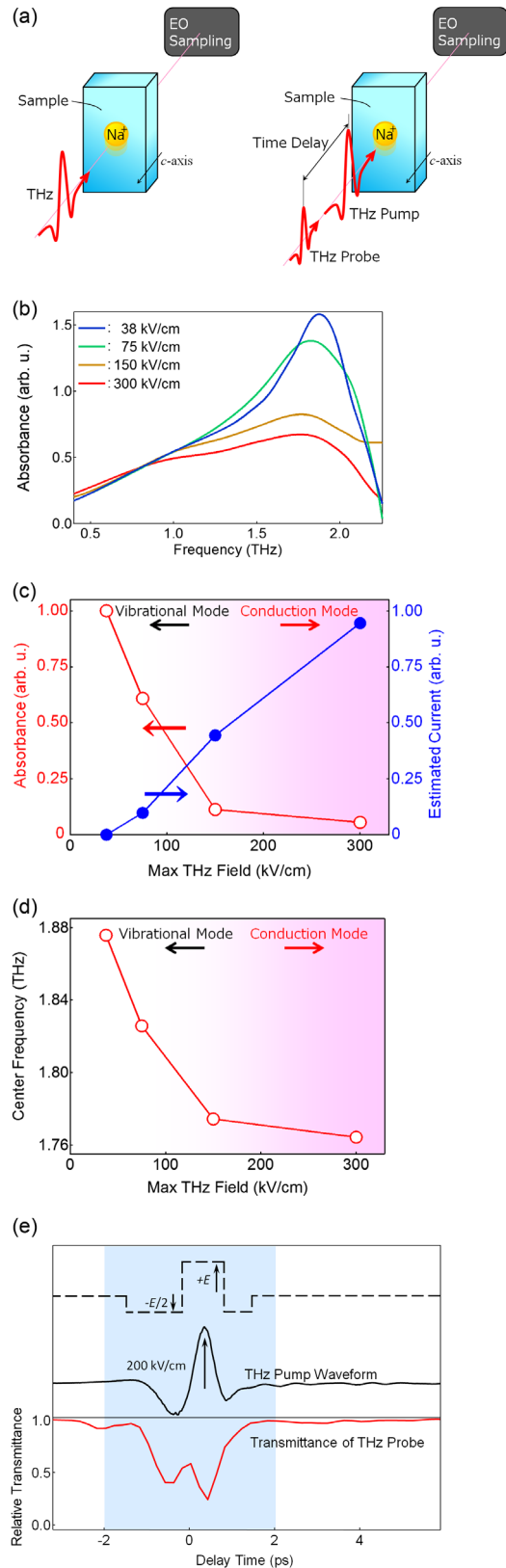


FIG. 2. Response of an ion in the sample under terahertz-field illumination. (a) Terahertz intensity dependence of the ionic current averaged  $10^3$  times, measured using an ammeter. The current direction changes based on the polarity of the terahertz field. The solid curve is the best fit of Eq. (1). (b) Configuration of the ion and local potential in real space for  $\text{Na}^+$   $\beta$ -alumina at room temperature. The left side of the figure shows the  $\text{Na}^+$  ion in the vibrational mode under weak terahertz-field illumination, whereas the right side shows the ion in the conduction mode under intense terahertz-field illumination.

absorbance and center frequency associated with the  $\text{Na}^+$  ion vibrations, as shown in Figs. 3(c) and 3(d), respectively. Here, to isolate the contribution of the vibrational mode, we performed the fitting using two Gaussian curves: one was used for evaluating the vibrational mode with a center frequency of approximately 1.8 THz, and the other was used for evaluating the broad background with a center frequency of  $\sim 1.2$  THz. Although the origin of the background remains unclear, we found that neither the absorbance nor the center frequency of the mode at 1.2 THz depend on the terahertz field strength, implying that the background is independent of the terahertz-field-induced phenomena. The peak absorbance for fields greater than 150 kV/cm is almost ten times lower than that for a field of 38 kV/cm. As the peak absorbance is proportional to the density of the trapped  $\text{Na}^+$  ions, this result implies that most of the  $\text{Na}^+$  ions are promoted to the conduction mode when the peak terahertz field exceeds 150 kV/cm. Assuming that all the  $\text{Na}^+$  ions are in the vibrational mode under a weak electric field of 38 kV/cm and in the conduction mode under a high electric field of 300 kV/cm, the terahertz-field-induced current is proportional to the fraction of  $\text{Na}^+$  ions in the conduction mode multiplied by the terahertz field strength. Figure 3(c) shows the plot of the terahertz-induced current with respect to



the change in the absorbance, indicating a strong correlation between these phenomena. In addition, a slight frequency softening of the absorption peak is observed [see Fig. 3(d)], which is expected as the shape of the energy potential has a smaller slope at high energies. From the spectral analyses shown in Figs. 3(c) and 3(d), the spectral change, shown in Fig. 3(b), provides a strong evidence for the terahertz-field-induced ionic motion. As the terahertz-induced current is also proportional to the distance traveled by the ions from their original positions, the total time during which the ions remain mobile is significant. To experimentally investigate the total time, we employed intense terahertz pump–terahertz probe spectroscopy [see the right portion of Fig. 3(a)]. The peak terahertz electric field of the probe beam is approximately 5 kV/cm, which is weak enough to avoid the stimulation of Na<sup>+</sup> ion motion. Figure 3(e) shows the time dependence of the transmittance intensity of the terahertz probe pulse averaged over a frequency range of 0.4–2.2 THz as a function of the pump–probe delay. The middle of the figure shows the terahertz pump waveform. As shown in this

FIG. 3. (a) Outline of the experimental setup of terahertz time-domain spectroscopy. The generated terahertz field is incident on the sample, and the transmitted field is measured using an electro-optic (EO) sampling method (left side). The terahertz pump–terahertz probe spectroscopy used in this study is shown on the right side of (a). The experiments shown in (a) are carried out under a nitrogen atmosphere at room temperature. (b) Terahertz intensity dependence of the absorbance for the sample. The peak at 1.8 THz corresponds to Na<sup>+</sup> ion vibrations; the peak vanishes as the terahertz field becomes more intense. (c) Terahertz intensity dependence of the normalized absorbance of Na<sup>+</sup> ions (red line and open circle). As the terahertz field becomes more intense, the absorbance decreases drastically, implying that the ions are trapped in their local potentials under weak terahertz fields, whereas they escape from their local potentials under intense terahertz fields. In other words, the motion of Na<sup>+</sup> ions changes from a vibrational mode to a conduction mode. The terahertz intensity dependence of the current obtained by an estimation stated in the main text is also shown in this figure (blue line with solid circles); the results are in good qualitative agreement with that shown in Fig. 2(a). (d) Terahertz intensity dependence of the center frequency of the Na<sup>+</sup> ion absorption. The center frequency decreases as the terahertz field becomes more intense. (e) Relative terahertz transmittance measured using intense terahertz pump–terahertz probe spectroscopy. The transmittance of the probe terahertz pulse decreases only when the sample is illuminated by an intense terahertz field (shaded area), implying that the ions move only when the pump terahertz field is incident on the sample. The scaled terahertz electric field with a square waveform used for the calculation is also shown.

figure, the transmittance decreases only when the electric field of the terahertz pump is sufficiently high regardless of the polarity of the terahertz pulse and recovers immediately ( $\sim$ sub-ps timescale) following terahertz pump illumination. The lack of change in the transmittance with respect to the zero time suggests that the conductivity changes only when the terahertz pump is present and that the ions remain trapped in the absence of the field. From the above results, the mechanism involved in the current generation can be qualitatively understood as follows. In the absence of a terahertz field, the  $\text{Na}^+$  ions are trapped in the periodic potential minima in the lattice. If the  $\text{Na}^+$  ions are not given sufficient energy to overcome the potential barrier, the ions will vibrate at the bottom of the potential well, as shown in the left portion of Fig. 2(b), and no current will be detected. However, with a high terahertz field, the vibrational frequency decreases because of the anharmonicity brought on by the cosine shape of the energy potential. If the additional energy provided by the terahertz field is sufficient to overcome the potential barrier, the  $\text{Na}^+$  ions will be transported until the supplied energy is relaxed. The net current can be detected using a conventional ammeter.

To understand the observed ion dynamics, we examined two simple simulation models: a standard transport model based on the equation of motion of  $\text{Na}^+$  ions (Supplemental Material [18]) and a thermally excited transport model [25]. The former model can qualitatively explain the ion dynamics, particularly the time transient of the position in real space (Fig. 1S). However, this model predicts much higher field ( $\sim 30$  MV/cm) for the delocalization of  $\text{Na}^+$  ions than the experimentally observed depinning field ( $\sim 50$  kV/cm), whose discrepancy might come from factors excluded from the model such as thermal activation of  $\text{Na}^+$  ions and many-body effects. In the latter model, therefore, we introduce the thermally excited current driven by the terahertz electric field expressed by

$$I(E) = f_{\text{rep}} \times \int S n \beta q \Lambda \nu \exp\left(-\frac{V_0}{k_B T}\right) \times 2 \sinh\left(\frac{\beta q \Lambda E(t)}{2 k_B T}\right) dt, \quad (1)$$

where  $S$  ( $=1 \text{ mm} \times 23 \text{ }\mu\text{m}$ ) is the cross section of the sample,  $n$  ( $=1 \times 10^{25} \text{ m}^{-3}$  [26]) is the  $\text{Na}^+$  ion density,  $\beta$  is the adjustable effective factor [27,28],  $q = e$  ( $>0$ ) is the charge on the  $\text{Na}^+$  ions,  $\Lambda$  ( $=6.4 \text{ \AA}$ ) is the potential period [14],  $\nu$  ( $=1.8 \text{ THz}$ ) is the vibrational frequency of the  $\text{Na}^+$  ions,  $V_0$  ( $=0.5 \text{ eV}$ ) is the height of the potential barrier [14],  $k_B$  is the Boltzmann constant,  $T$  ( $=290 \text{ K}$ ) is the lattice temperature, and  $E(t)$  is the applied electric field. The electric field modifies the height of the potential barrier by  $-q(\Lambda/2)E$  [ $+q(\Lambda/2)E$ ] for [against] the electric field, and resultantly, the mean velocity of the ion is given by  $\Lambda \nu \exp(-V_0/k_B T) \times 2 \sinh(q\Lambda E/2k_B T)$ , where

$\nu \exp(-V_0/k_B T)$  corresponds to the frequency factor that thermally climbs over the potential barrier. The effective parameter  $\beta$  modifies either the charge or the potential period, i.e., hopping length of the  $\text{Na}^+$  ions. Here, we simply assume that the terahertz electric field has a positive and negative oscillatory square waveform with 3 ps as shown by a broken line in Fig. 3(e). By taking the square-shaped terahertz electric field with a repetition rate of 1 kHz ( $f_{\text{rep}} = 1 \text{ kHz}$ ) into consideration, we could remove the direct-current components from our analysis and simply calculate the total current  $I(E)$ . By using the parameter value of  $\beta = 62$ , we could quantitatively reproduce the experimental data as shown by a solid curve in Fig. 2(a). The large value of  $\beta$  implies that either the charge or the hopping length is somewhat enhanced due to implicit factors such as collective and many-body effects. Despite the simplicity of our simulation models, most of the experimental results could be reproduced, and the models can provide useful insight into the underlying physics of ion dynamics in superionic conductors; the standard transport model based on the equation of motion provides the qualitative ionic dynamics in real space, while the thermally excited current model numerically reproduces the macroscopic ionic current induced by the applied terahertz electric field. The obtained experimental and simulation results strongly suggest that the ions in a superionic conductor can be driven nonperturbatively to induce a current and that the ions travel several nanometers on subpicosecond timescales.

In conclusion, we experimentally accelerated the ions in a  $\text{Na}^+$   $\beta$ -alumina superionic conductor by applying intense terahertz fields and measured the induced macroscopic direct current. Through terahertz time-domain spectroscopy measurements, we observed a reduction in the vibrational absorption because of the absence of vibrating ions. In addition, we implemented two simple analyses to understand the observed ion dynamics. By using the equation of motion of  $\text{Na}^+$  ions, we could simulate ion movements in real space and clarified that the response of  $\text{Na}^+$  ions to the terahertz field was due to a change in their dynamics from a vibrational mode to a conduction mode. By calculating the thermally excited current driven by the terahertz electric field, the terahertz-field-induced macroscopic current could be semi-quantitatively explained using the enhancement factor of  $\beta$ . Although a sophisticated theory to quantitatively explain the overall ion dynamics is still required, we believe that our finding—macroscopic current flow in a superionic conductor driven by single-cycle terahertz pulses—may pave the way for future ultrafast ionics.

This work was supported in part by the Grants-in-Aid for Scientific Research (KAKENHI, No. 17H06124, No. 18H04288, and No. 19K03701) from the Japan Society for the Promotion of Science (JSPS). The research at MIT was supported in part by U.S. NSF Grant No. CHE-1665383.

\* minami@tokushima-u.ac.jp

- [1] P. B. Corkum and F. Krausz, *Nat. Phys.* **3**, 381 (2007).
- [2] M. Krüger, M. Schenk, and P. Hommelhoff, *Nature (London)* **475**, 78 (2011).
- [3] A. Schiffrin *et al.*, *Nature (London)* **493**, 70 (2013).
- [4] F. Krausz and M. I. Stockman, *Nat. Photonics* **8**, 205 (2014).
- [5] L. Wimmer, G. Herink, D. R. Solli, S. V. Yalunin, K. E. Echternkamp, and C. Ropers, *Nat. Phys.* **10**, 432 (2014).
- [6] T. Rybka, M. Ludwig, M. F. Schmalz, V. Knittel, D. Brida, and A. Leitenstorfer, *Nat. Photonics* **10**, 667 (2016).
- [7] A. V. Kolobov, P. Fons, A. I. Frenkel, A. L. Ankudinov, J. Tominaga, and T. Uruga, *Nat. Mater.* **3**, 703 (2004).
- [8] K. Yoshioka, I. Katayama, Y. Minami, M. Kitajima, S. Yoshida, H. Shigekawa, and J. Takeda, *Nat. Photonics* **10**, 762 (2016).
- [9] Y. Kato, S. Hori, T. Saito, K. Suzuki, M. Hirayama, A. Mitsui, M. Yonemura, H. Iba, and R. Kanno, *Nat. Energy* **1**, 16030 (2016).
- [10] B. N. Pal, B. M. Dhar, K. C. See, and H. E. Katz, *Nat. Mater.* **8**, 898 (2009).
- [11] B. L. Ellis, W. R. M. Makahnouk, Y. Makimura, K. Toghill, and L. F. Nazar, *Nat. Mater.* **6**, 749 (2007).
- [12] N. Yabuuchi, M. Kajiyama, J. Iwatate, H. Nishikawa, S. Hitomi, R. Okuyama, R. Usui, Y. Yamada, and S. Komaba, *Nat. Mater.* **11**, 512 (2012).
- [13] X. Wang, S. Kajiyama, H. Iinuma, E. Hosono, S. Oro, I. Moriguchi, M. Okubo, and A. Yamada, *Nat. Commun.* **6**, 6544 (2015).
- [14] G. Lucazeau, *Solid State Ionics* **8**, 1 (1983).
- [15] J. R. Walker and C. R. A. Catlow, *J. Phys. C* **15**, 6151 (1982).
- [16] J. Hebling, G. Almási, I. Z. Kozma, and J. Kuhl, *Opt. Express* **10**, 1161 (2002).
- [17] H. Hirori, A. Doi, F. Blanchard, and K. Tanaka, *Appl. Phys. Lett.* **98**, 091106 (2011).
- [18] See Supplemental Material at <http://link.aps.org/supplemental/10.1103/PhysRevLett.124.147401> for details of the ion dynamics, particularly the time transient of the position in real space, and the spectrum change induced by intense terahertz fields, which includes Refs. [19–24].
- [19] P. Colomban and G. Lucazeau, *J. Chem. Phys.* **72**, 1213 (1980).
- [20] W. Kuehn, P. Gaal, K. Reimann, M. Woerner, T. Elsaesser, and R. Hey, *Phys. Rev. Lett.* **104**, 146602 (2010).
- [21] T. Shih, K. Reimann, M. Woerner, T. Elsaesser, I. Waldmüller, A. Knorr, R. Hey, and K. H. Ploog, *Phys. Rev. B* **72**, 195338 (2005).
- [22] Y. Minami, K. Araki, T. D. Dao, T. Nagao, M. Kitajima, J. Takeda, and I. Katayama, *Sci. Rep.* **5**, 15870 (2015).
- [23] U. Strom, P. C. Taylor, S. G. Bishop, T. L. Reinecke, and K. L. Ngai, *Phys. Rev. B* **13**, 3329 (1976).
- [24] A. S. Barker, Jr., J. A. Ditzenberger, and J. P. Remeika, *Phys. Rev. B* **14**, 4254 (1976).
- [25] N. F. Mott and R. W. Gurney, *Electronic Processes in Ionic Crystals* (Dover, New York, 1948), Chap. II.
- [26] K. L. Ngai and U. Strom, *Phys. Rev. B* **38**, 10350 (1988).
- [27] I. Katayama, H. Aoki, J. Takeda, H. Shimosato, M. Ashida, R. Kinjo, I. Kawayama, M. Tonouchi, M. Nagai, and K. Tanaka, *Phys. Rev. Lett.* **108**, 097401 (2012).
- [28] B. E. Knighton, R. T. Hardy, C. L. Johnson, L. M. Rawlings, J. T. Woolley, C. Calderon, A. Urrea, and J. A. Johnson, *J. Appl. Phys.* **125**, 144101 (2019).